J. Fluid Mech. (1972), *vol.* 52, *part* 1, *pp.* 161–177
Printed in Great Britain

Flow patterns in models of small airway units of the lung

By M. R. DAVIDSON AND J. M. FITZ-GERALD
Department of Mathematics, University of Queensland, Australia

(Received 2 August 1971)

Quasi-steady creeping flow in models of small airway units of the lung is investigated. A respiratory unit of the lung is modelled by a sphere, an oblate and a prolate ellipsoid of revolution, and a circular cylinder of finite length. The solution of the Stokes equations for each of these geometries is indicated for general axisymmetric boundary conditions. For particular cases consistent with the models, streamlines are plotted and some velocity profiles are shown. It is suggested that bulk flow in the final generations of the lung is significant for gas transport even though diffusion is the predominant mechanism there.

1. Introduction

The airways of the human lung begin with a single tube, the trachea, which divides into a right and a left principal bronchus, each bronchus supplying a half lung. Subsequent branches to about the 10th generation, where the diameter has decreased to about 1 mm, are termed bronchi. Branching continues with a series of airways called bronchioles. At about the 17th generation, where a typical airway diameter is 0·5 mm, the bronchioles begin to acquire alveoli – outpouchings where gas exchange occurs – and are hence called respiratory bronchioles. The degree of alveolation increases with generation until about the 20th, where the airways (alveolar ducts) are completely surrounded by alveoli. The whole system of branching terminates at about the 23rd generation with enclosures called alveolar sacs. These sacs also bear alveoli and, like the alveolar ducts, have no real walls but are open on all sides to alveoli.

Gas exchange occurs across the alveolar walls, which enclose a dense network of capillaries; O_2 diffuses into the blood and CO_2 is released into the alveoli. Gas transport in the lungs between the upper respiratory regions and the alveolar walls depends on both convection and diffusion. In the larger airways (trachea and bronchi) convection dominates; mixing occurs in the secondary flows at branchings and assists in the distribution of oxygen during inspiration. As the total airway cross-sectional area increases, and velocities correspondingly decrease, diffusion assumes an increasingly important role. However, the adequate distribution of gases to all sections of the final alveolated generations may still depend significantly on the convection process, as discussed later.

The object of this paper is to study the convective flow in various models of a respiratory unit consisting of an alveolar duct together with its surrounding alveoli. Streamlines are plotted and some velocity profiles are shown.

2. Models of a respiratory unit

The usual classification of the final branchings of the lung as ducts and alveoli is not suitable for a discussion of the flows therein. The equations of motion are elliptic; the flow is therefore determined by the geometry of the whole space available. Rather than considering a (non-existent) well-defined central duct carrying a flow which is perturbed by alveolar openings, it is preferable to think in terms of a single 'respiratory unit' containing partitions which define the individual alveoli. Such partitions are henceforth referred to as interalveolar partitions since any one of them is a wall common to adjacent alveoli. Altshuler (1968) also observed the desirability of treating the alveolar duct and its alveoli as a single entity and correspondingly defined an 'alveolar spatial unit'.

Studying the flow through a respiratory unit is too difficult unless considerable simplifications are made. It is convenient to neglect the interalveolar partitions (the effects of doing this are discussed later) and then model the unit with a number of axially symmetric figures (see figure 1). The cases considered include models with stationary and with expanding walls.

2.1. *Flow equations*

In the small airways the Mach number is very small, and changes in air density caused by molecular diffusion of O_2 and CO_2 are negligible since N_2 is the major constituent; the flow is effectively incompressible. Therefore, incorporating body forces in the pressure term, the equations of motion are

$$\frac{\partial \mathbf{u}}{\partial t} + \mathbf{u}.\nabla\mathbf{u} + \frac{\nabla p}{\rho} = \nu\nabla^2\mathbf{u}, \quad \nabla.\mathbf{u} = 0,$$

where $\mathbf{u}$ is the fluid velocity, p is the modified pressure, ρ is the density and ν is the kinematic viscosity. If we non-dimensionalize the variables in the equations as follows:

$$t^* = t/T, \quad \mathbf{u}^* = \mathbf{u}/U,$$

$$\mathbf{x}^* = \mathbf{x}/D, \quad (p/\rho)^* = \frac{p/\rho}{\nu U/L},$$

where D, U and T are some characteristic length, velocity and time respectively, the equations become

$$\frac{D^2}{\nu T}\frac{\partial \mathbf{u}^*}{\partial t^*} + \frac{UD}{\nu}\mathbf{u}^*.\nabla^*\mathbf{u}^* + \nabla^*\left(\frac{p}{\rho}\right)^* = \nabla^{*2}\mathbf{u}^*.$$

The Reynolds number, $R = UD/\nu$, is small ($R = 0{\cdot}056$, based on an average velocity $U = 0{\cdot}1$ cm/s and a typical unit diameter $D = 900\,\mu$m), so that the non-linear inertia term $\mathbf{u}.\nabla\mathbf{u}$ in the flow equations may be neglected. Another dimensionless parameter, $P = D^2/\nu T$, must be considered for the unsteady flows in a respiratory unit which result from the act of breathing. T is some typical period of the unsteady motion, in this case the time for a single breath. P is small ($P = 0{\cdot}013$, based on $D = 900\,\mu$m and $T = 4$ s), therefore the term $\partial\mathbf{u}/\partial t$ may be neglected in the flow equations and the flow is quasi-steady.

The equations of motion are now the Stokes flow equations (with an implicit time variable), which, in the axisymmetric case, may be reduced to the single equation

$$D^4\psi = 0, \tag{1}$$

where ψ is the Stokes stream function and the form of the differential operator D^2 varies with the co-ordinate system used. Each problem is rendered dimensionless using length L (see figure 1) and U_0, the instantaneous maximum entrance velocity with respect to the model.

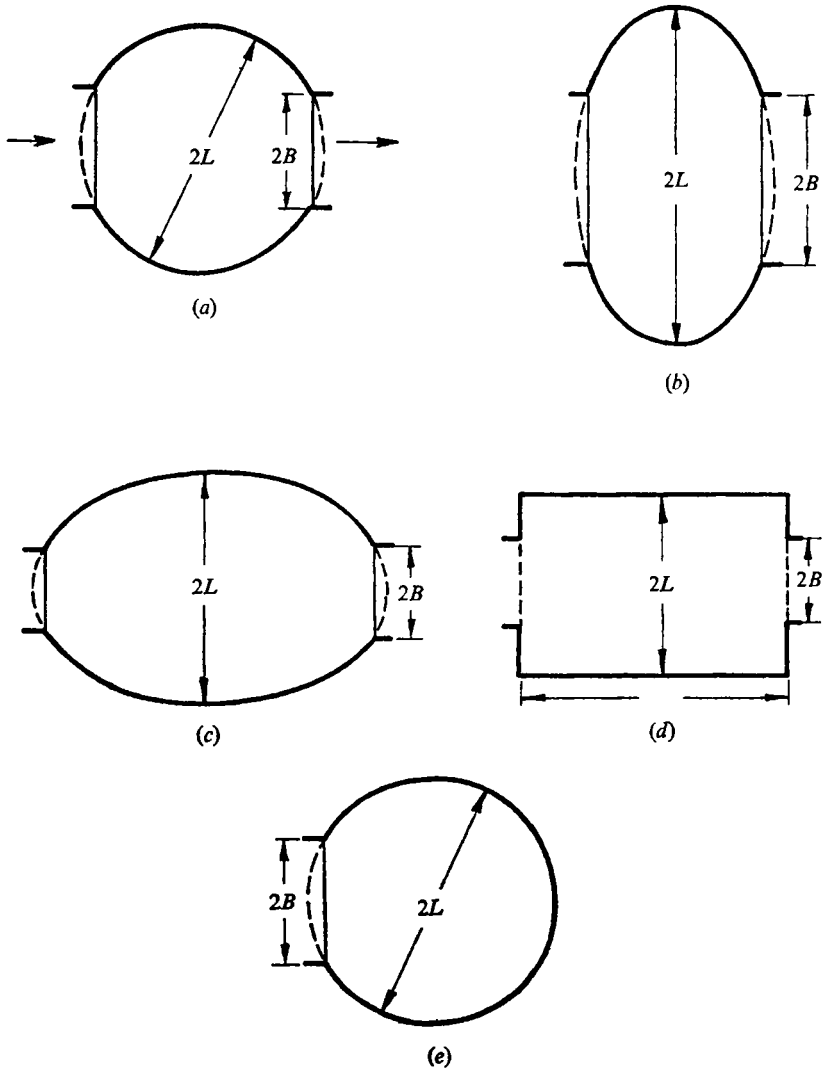

FIGURE 1. Models of a respiratory unit with a circular section removed from one or both ends. Broken lines are the regions upon which the end velocity conditions are imposed. (*a*) Sphere, (*b*) oblate ellipsoid of revolution, (*c*) prolate ellipsoid of revolution, (*d*) circular cylinder, (*e*) sphere.

2.2. *Co-ordinate systems*

Let σ and x be the familiar cylindrical co-ordinates where x is the axis of symmetry of any figure. Choose the origin at the centre of the figure for any geometry. For a particular geometry a co-ordinate system is chosen so that one of the co-ordinates remains constant on the boundary; e.g. cylindrical co-ordinates are used for the circular cylinder because σ is constant on the cylinder. For the sphere, spherical co-ordinates (r, θ) are used where θ is the angle between radius r and the positive x axis and we define $\mu = \cos\theta$. For the oblate ellipsoid of revolution, oblate spheroidal co-ordinates (η, θ), given by

$$\sigma = c\cosh\eta\sin\theta \quad \text{and} \quad x = c\sinh\eta\cos\theta,$$

where c is a positive constant, $0 \leqslant \eta < \infty$ and $0 \leqslant \theta \leqslant \pi$, are used. If $\lambda = \sinh\eta$ then $\sigma = c[(1+\lambda^2)(1-\mu^2)]^{\frac{1}{2}}$ and $x = c\lambda\mu$. In a similar way the co-ordinates for the prolate ellipsoid of revolution are $\sigma = c[(\gamma^2-1)(1-\mu^2)]^{\frac{1}{2}}$ and $x = c\gamma\mu$, where $\gamma = \cosh\eta$.

2.3. *Axisymmetric flow in a sphere*

On $r = 1$ general boundary conditions for flow axisymmetric about the x axis are

$$u_r = F(\mu), \quad u_\theta = -\sin\theta G(\mu), \quad u_\phi = 0,$$

where u_r, u_θ and u_ϕ are the velocity components in spherical co-ordinates. The total flux across the surface of the sphere is zero, so

$$\int_{-1}^{1} F(\mu)\,d\mu = 0.$$

We now introduce the Stokes stream function $\psi(r, \theta)$ given, in these co-ordinates, by

$$u_r = \frac{1}{r^2\sin\theta}\frac{\partial\psi}{\partial\theta}, \quad u_\theta = -\frac{1}{r\sin\theta}\frac{\partial\psi}{\partial r},$$

with $\psi(r, \theta)$ zero on the axis of symmetry, x. The boundary conditions on $r = 1$ become

$$\psi = -\int_{-1}^{\mu} F(t)\,dt = f(\mu), \quad \text{say,} \tag{2}$$

and

$$\frac{\partial\psi}{\partial r} = (1-\mu^2)G(\mu) = g(\mu), \quad \text{say.} \tag{3}$$

Note that (2) gives $\psi = 0$ on $\mu = +1$ as desired.

In spherical co-ordinates

$$D^2 = \frac{\partial^2}{\partial r^2} + \frac{1-\mu^2}{r^2}\frac{\partial^2}{\partial\mu^2}$$

and (1) has a solution of the general form

$$\psi(r, \theta) = \sum_{n=0}^{\infty}(A_n r^{n+1} + B_n r^{-n} + C_n r^{n+3} + D_n r^{-n+2})\,T_n(\mu), \tag{4}$$

where, if $P_n(\mu)$ is a Legendre polynomial of degree n,

$$T_n(\mu) = \int_{-1}^{\mu} P_n(t)\,dt.$$

Requiring ψ, u_r and u_θ to be finite at the origin and ψ to be zero on $\mu = \pm 1$ reduces (4) to

$$\psi(r, \theta) = \sum_{n=1}^{\infty} (A_n r^{n+1} + C_n r^{n+3}) T_n(\mu).$$

Applying the boundary conditions (2) and (3) yields

$$\sum_{n=1}^{\infty} (A_n + C_n) T_n(\mu) = f(\mu) \tag{5}$$

and

$$\sum_{n=1}^{\infty} [(n+1) A_n + (n+3) C_n] T_n(\mu) = g(\mu). \tag{6}$$

If

$$E_{n,m} = \int_{-1}^{1} t^n T_m(t)\, dt$$

then

$$E_{n,m} = \frac{1}{n+1} (2\delta_{m0} - I_{n+1,m}),$$

where

$$I_{n,m} = \int_{-1}^{1} t^n P_m(t)\, dt$$

and, from Whittaker & Watson (1952),

$$I_{n,m} \begin{cases} = \dfrac{2^{m+1} n! \left(\frac{1}{2}(n+m)\right)!}{\left(\frac{1}{2}(n-m)\right)! (n+m+1)!} & \text{for } n-m \text{ even and non-negative,} \\ = 0 \quad \text{otherwise.} \end{cases}$$

So $E_{k,n} = -I_{k+1,n}/(k+1)$ for $n \neq 0$ and is non-zero only for $(k+1-n)$ even and non-negative.

Thus multiplying (5) and (6) by μ^k (with k an integer) and integrating gives

$$\sum_{n=1}^{k+1} (A_n + C_n) E_{k,n} = F_k$$

and

$$\sum_{n=1}^{k+1} [(n+1) A_n + (n+3) C_n] E_{k,n} = G_k,$$

where

$$F_k = \int_{-1}^{1} \mu^k f(\mu)\, d\mu \quad \text{and} \quad G_k = \int_{-1}^{1} \mu^k g(\mu)\, d\mu.$$

By successively setting $k = 0, 2, 4, \ldots$, we can obtain as many coefficients for odd n as we wish. Similarly by setting $k = 1, 3, 5, \ldots$ we can obtain the coefficients for even n. We should note, however, that in cases where the flow is symmetric all coefficients for even n will be zero.

2.4. *Axisymmetric flow in an oblate ellipsoid of revolution*

If $\eta = \eta_0$ on the boundary, then the length of the semi-major axis is $c \cosh \eta_0$, which equals unity, and $\lambda = (1 - c^2)^{\frac{1}{2}}/c = \lambda_0$, say, on the boundary. On $\lambda = \lambda_0$, general boundary conditions for flow, axisymmetric about the x axis, are

$$u_\eta = F(\mu), \tag{7}$$

$$u_\theta = -\sin\theta G(\mu), \tag{8}$$

$$u_\phi = 0,$$

where u_η, u_θ and u_ϕ are velocity components in oblate spheroidal co-ordinates.

The total flux across the surface of the figure is zero, so

$$\int_{-1}^{1} (1-c^2+c^2\mu^2)^{\frac{1}{2}} F(\mu)\, d\mu = 0.$$

In these co-ordinates the Stokes stream function is given by

$$u_\eta = \frac{1}{(c^2 \cosh\eta \sin\theta\, (\cosh^2\eta - \sin^2\theta)^{\frac{1}{2}})} \frac{\partial\psi}{\partial\theta}$$

and

$$u_\theta = \frac{-1}{(c^2 \cosh\eta \sin\theta\, (\cosh^2\eta - \sin^2\theta)^{\frac{1}{2}})} \frac{\partial\psi}{\partial\eta},$$

with $\psi(\eta, \theta) = 0$ on the axis of symmetry x. The boundary conditions on $\lambda = \lambda_0$ become

$$\psi = -\int_{-1}^{\mu} (1-c^2+c^2t^2)^{\frac{1}{2}} F(t)\, dt = f(\mu), \quad \text{say} \tag{9}$$

and

$$\partial\psi/\partial\lambda = c(1-\mu^2)\,(1-c^2+c^2\mu^2)^{\frac{1}{2}} G(\mu) = g(\mu), \quad \text{say.} \tag{10}$$

In these co-ordinates

$$D^2 = \frac{1}{c^2(\lambda^2+\mu^2)} \left((1+\lambda^2) \frac{\partial^2}{\partial\lambda^2} + (1-\mu^2) \frac{\partial^2}{\partial\mu^2} \right)$$

and (1) has a solution of the general form

$$\psi = \sum_{n=0}^{\infty} (A_n W_n(\mu, -i\lambda) + B_n T_n(\mu) T_n(-i\lambda)), \tag{11}$$

where

$$W_n(\mu, z) = \frac{(n+2)(n+3)}{(2n+3)^2} (T_n(\mu) T_{n+2}(z) + T_n(z) T_{n+2}(\mu)) - \frac{(n-1)(n+3)}{(2n-1)^2} (T_n(\mu) T_{n-2}(z) + T_n(z) T_{n-2}(\mu)) \quad \text{for} \quad n \geqslant 1$$

and

$$W_0(\mu, z) = 2(T_0(\mu) T_1(z) + T_0(z) T_1(\mu)) + \tfrac{2}{3}(T_0(\mu) T_2(z) + T_0(z) T_2(\mu)).$$

However, since ψ must be zero on $\mu = \pm 1$, A_0 and B_0 are both zero. Applying the boundary conditions (9) and (10) yields

$$\sum_{n=1}^{\infty} (A_n W_n(\mu, -i\lambda_0) + B_n T_n(\mu) T_n(-i\lambda_0)) = f(\mu) \tag{12}$$

and

$$\sum_{n=1}^{\infty} (A_n W_n'(\mu, i\lambda_0) + B_n T_n(\mu) T_n'(-i\lambda_0)) = g(\mu), \tag{13}$$

where a prime indicates differentiation with respect to λ.

Now define

$$W_{k,n}(z) = \int_{-1}^{1} \mu^k W_n(\mu, z)\, d\mu \quad \text{for} \quad n \geqslant 1.$$

So

$$W_{k,n}(z) = \frac{(n+2)(n+3)}{(2n+3)^2} (E_{k,n} T_{n+2}(z) + E_{k,n+2} T_n(z)) - \frac{(n-1)(n-2)}{(2n-1)^2} (E_{k\ n} T_{n-2}(z) + E_{k,n-2} T_n(z))$$

and is non-zero only for $(k+3-n)$ even and non-negative. Multiplying (12) and (13) by μ^k, integrating and using the properties of $W_{k,n}$ and $E_{k,n}$ gives

$$\sum_{n=1}^{k+3} A_n W_{k,n}(-i\lambda_0) + \sum_{n=1}^{k+1} B_n T_n(-i\lambda_0) E_{k,n} = F_k$$

and $$\sum_{n=1}^{k+3} A_n W'_{k,n}(-i\lambda_0) + \sum_{n=1}^{k+1} B_n T'_n(-i\lambda_0) E_{k,n} = G_k.$$

Let k be even and consider the system

$$\sum_{n=3}^{k+3} A_n W_{k,n}(-i\lambda_0) + \sum_{n=1}^{k+1} B_n T_n(-i\lambda_0) E_{k,n} = F_k, \tag{14}$$

$$\sum_{n=3}^{k+3} A_n W'_{n,k}(-i\lambda_0) + \sum_{n=1}^{k+1} B_n T'_n(-i\lambda_0) E_{k,n} = G_k. \tag{15}$$

By successively setting $k = 0, 2, 4, \ldots$, solutions of (14) and (15), A_n^* for $n = 3, 5, 7, \ldots$ and B_n^* for $n = 1, 3, 5, \ldots$ may be obtained up to any odd value of n. If F_k and G_k are replaced in (14) and (15) by $W_{k,1}(-i\lambda_0)$ and $W'_{k,1}(-i\lambda_0)$ respectively and solutions $\bar{A}_n$ and $\bar{B}_n$ are obtained, then for odd n the actual coefficients in the eigenfunction expansion for ψ will have the form

$$\begin{aligned} A_n &= A_n^* - A_1 \bar{A}_n \quad (n = 3, 5, 7, \ldots), \\ B_n &= B_n^* - A_1 \bar{B}_n \quad (n = 1, 3, 5, \ldots). \end{aligned} \tag{16}$$

Similarly, by making k odd, A_n and B_n will have the following form for even n:

$$\begin{aligned} A_n &= A_n^* - A_2 \bar{A}_n \quad (n = 4, 6, 8, \ldots), \\ B_n &= B_n^* - A_2 \bar{B}_n \quad (n = 2, 4, 6, \ldots). \end{aligned} \tag{17}$$

We now truncate the series for ψ after N terms, substitute the expressions (16) and (17) into (11) and match the truncated series with $f(\mu)$ at the boundary $\lambda = \lambda_0$ by means of a least-squares criterion. This procedure will produce estimates for A_1 and A_2. Again, if the flow is symmetric, all coefficients for even n are zero.

2.5. *Axisymmetric flow in a prolate ellipsoid of revolution*

The semi-minor axis of the ellipsoid of revolution has length unity, so if $\gamma = \gamma_0$ on the boundary, then $\gamma_0 = (1+c^2)^{\frac{1}{2}}/c$. The boundary conditions on $\gamma = \gamma_0$ are (7) and (8) together with $u_\phi = 0$, and the solution has the form

$$\psi = \sum_{n=1}^{\infty} (A_n W_n(\mu, \gamma) + B_n T_n(\mu) T_n(\gamma)).$$

The coefficients may be obtained from the boundary conditions in the manner of the previous section.

2.6. *Axisymmetric flow in a circular cylinder of finite length*

This problem was investigated by Fitz-Gerald (1969) in order to examine the plasma flow in narrow capillaries. We use his solution, which involves expressing the stream function ψ in the form $\psi = \psi_p + \psi_a$, where ψ_p is the Poiseuille solution satisfying the no-slip conditions on $\sigma = 1$ and ψ_a is a solution selected to ensure that ψ satisfies the conditions at the ends. The selection is made by the choice of coefficients in the eigenfunction expansion for ψ_a.

3. Applications of the general solutions

Weibel (1963) mentions that in adults the total depth of the average alveolus is of the order of 250–300 μm, we therefore select

$$250 \leqslant L-B \leqslant 300\,\mu\text{m}. \tag{18}$$

The diameter of alveolar ducts and sacs varies between 200 and 600 μm, giving

$$100 \leqslant B \leqslant 300\,\mu\text{m}, \tag{19}$$

and the length-to-diameter ratio of alveolar ducts lies between 1 and 3, hence

$$1 \leqslant l/2B \leqslant 3, \tag{20}$$

where l is the length of the duct. From (18) and (19) we obtain

$$0{\cdot}25 \leqslant b \leqslant 0{\cdot}54. \tag{21}$$

The lengths of the respiratory units represented by figure 1 (*a*), (*b*), (*c*) and (*d*) are given by $l/L = 2(1-b^2)^{\frac{1}{2}}$, $l/L = 2[(1-c^2)(1-b^2)]^{\frac{1}{2}}$, $l/L = 2[(1+c^2)(1-b^2)]^{\frac{1}{2}}$ and $l/L = 2m$ respectively. Substitution into (20) gives a condition which must be satisfied simultaneously with (21) by the parameters involved.

For the circular cylinder of finite length the antisymmetric eigenfunctions decay at least as rapidly as $\sinh(\alpha_1 x)k(\sigma)$ away from the ends ($\alpha_1 \approx 4{\cdot}5 + i1{\cdot}5$) and cannot be associated with any net flow. Hence it is reasonable to assume symmetric boundary conditions (and hence symmetric flows) for those models with stationary walls. It should be noted however, that if the model is expanding, the flow cannot be symmetric.

Parabolic velocity conditions at the entrance and exit of the sphere (figure 1 (*a*)) with stationary walls are

$$u_x = 1-\sigma^2/b^2 \quad \text{and} \quad u_\sigma = 0 \quad \text{on} \quad r = 1 \quad \text{for} \quad (1-b^2)^{\frac{1}{2}} \leqslant |\mu| \leqslant 1.$$

By making use of the no-slip condition on the remainder of the sphere it is easy to show that

$$G(\mu)\begin{cases} = (1-1/b^2)+\mu^2/b^2 & \text{for} \quad (1-b^2)^{\frac{1}{2}} \leqslant |\mu| \leqslant 1, \\ = 0 \quad \text{elsewhere}, \end{cases}$$

and $F(\mu) = \mu G(\mu)$. To compare these with the parabolic velocity conditions we also consider a 'fourth-power' profile at the ends given by $u_x = 0{\cdot}75(1-\sigma^4/b^4)$ and $u_\sigma = 0$. We have chosen the maximum velocity to be 0·75 to ensure that the flux entering and leaving the sphere is the same for both 'fourth-power' and parabolic profiles; this provides a basis for comparison.

For Stokes flow, any entrance flow in a semi-infinite circular cylinder of radius unity decays to Poiseuille flow like $e^{-\alpha_1 x}k(\sigma)$, where x increases along the length of the pipe. Thus it requires very little distance along anything resembling a smooth-walled pipe between respiratory units for the flow to fall significantly to Poiseuille flow. Even if there is insufficient distance for this to occur, and the flow has decayed only as far as a 'fourth-power' profile say, figure 2 (*a*) shows that a large part of the flow in the unit is relatively unaffected by this difference in end profiles. It is therefore felt that the assumption of parabolic profiles at the

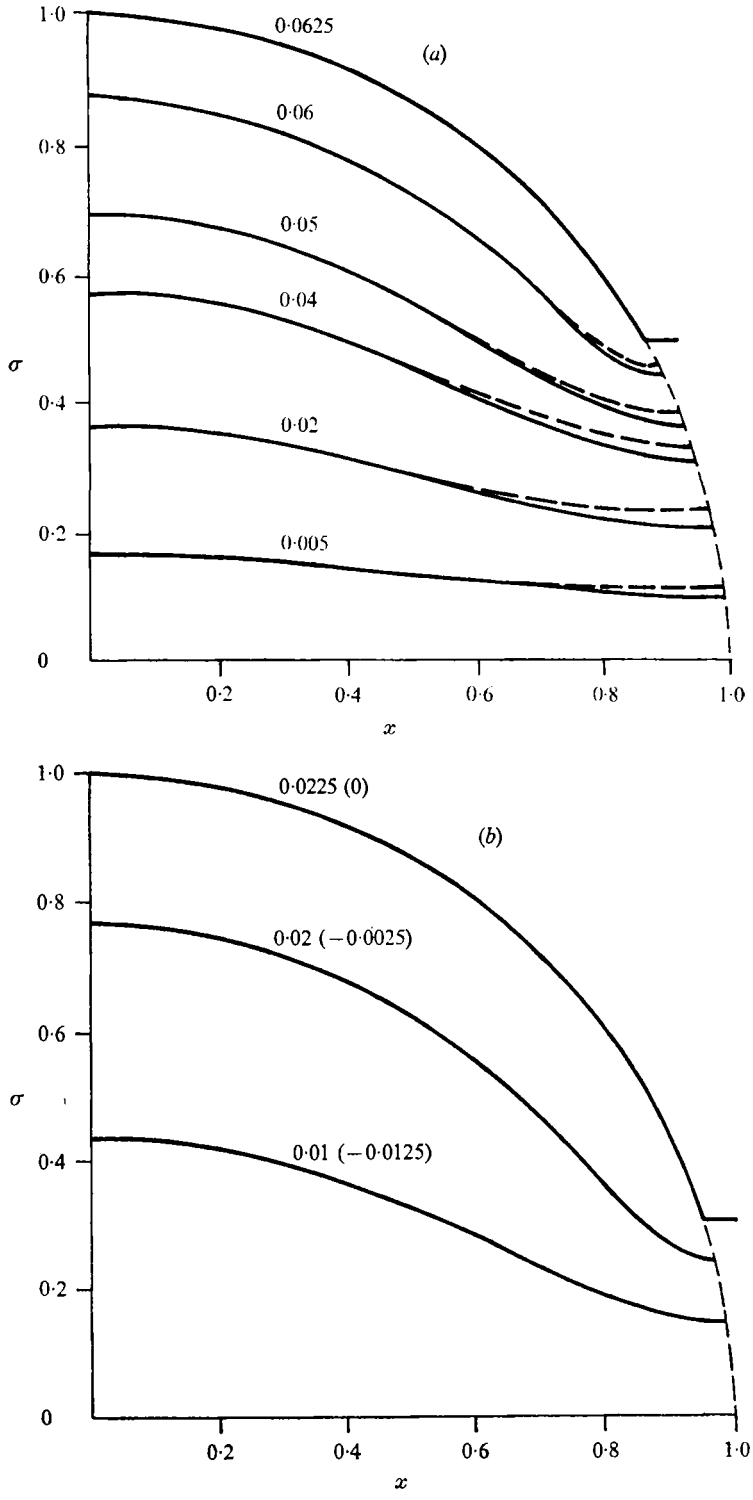

FIGURE 2. Streamlines in a quadrant of spherical model (*a*) with stationary walls. (*a*) $b = 0{\cdot}5$, broken lines are streamlines corresponding to the 'fourth-power' end velocity condition with the same flux. (*b*) $b = 0{\cdot}3$, bracketed numbers are the values of the stream function using the boundary as a reference line.

ends of model respiratory units will provide qualitative results characteristic of all end conditions which could occur, so parabolic end conditions are assumed for all geometries herein. In any case, the use of such idealized models precludes any more complicated assumptions.

Parabolic velocity conditions at the entrance and exit of the oblate ellipsoid of revolution (figure 1 (*b*)) with stationary walls, together with the no-slip condition on the remainder of the figure, gives

$$G(\mu)\begin{cases} = \left(\dfrac{1-c^2}{1-c^2+c^2\mu^2}\right)^{\frac{1}{2}}\left[\left(1-\dfrac{1}{b^2}\right)+\dfrac{\mu^2}{b^2}\right] & \text{for} \quad (1-b^2)^{\frac{1}{2}} \leqslant |\mu| \leqslant 1, \\ = 0 \quad \text{elsewhere}, \end{cases}$$

and $F(\mu) = (1-c^2)^{\frac{1}{2}}\mu G(\mu)$. Similarly for the prolate ellipsoid of revolution (figure 1 (*c*)) with stationary walls,

$$G(\mu)\begin{cases} = \left(\dfrac{1+c^2}{1+c^2-c^2\mu^2}\right)^{\frac{1}{2}}\left[\left(1-\dfrac{1}{b^2}\right)+\dfrac{\mu^2}{b^2}\right] & \text{for} \quad (1-b^2)^{\frac{1}{2}} \leqslant |\mu| \leqslant 1, \\ = 0 \quad \text{elsewhere}, \end{cases}$$

and $F(\mu) = (1+c^2)^{-\frac{1}{2}}\mu G(\mu)$. For the circular cylinder of finite length with stationary walls, $u_x = u_\sigma = 0$ on $\sigma = 1$, while on $x = \pm m$, $\mu_\sigma = 0$ and

$$u_x\begin{cases} = 1-(\sigma/b)^2 \quad \text{for} \quad \sigma \leqslant b, \\ = 0 \quad \text{elsewhere}. \end{cases}$$

For the sphere with expanding walls, parabolic entry and exit profiles with respect to the sphere are assumed, where U_0 and U_1 are the corresponding instantaneous maximum velocities. Let V be the instantaneous velocity of expansion, $v = V/U_0$ and $U = U_1/U_0$. Superimposing the Poiseuille velocities on the dimensionless radial velocity v at the ends we obtain

$$G(\mu)\begin{cases} = (1-1/b^2)+\mu^2/b^2 \quad \text{for} \quad -1 \leqslant \mu \leqslant (1-b^2)^{\frac{1}{2}}, \\ = U((1-1/b^2)+\mu^2/b^2) \quad \text{for} \quad (1-b^2)^{\frac{1}{2}} \leqslant \mu \leqslant 1, \\ = 0 \quad \text{elsewhere}, \end{cases}$$

and $F(\mu) = \mu G(\mu)+v$. Conservation of mass gives us $\frac{1}{4}b^2(1-U) = 2v$. Now, as the sphere expands, b will remain constant; so if we assume that U is a constant (that is, both U_0 and U_1 vary in the same way with time and differ only by a constant factor U) then v will be constant. For the sphere (figure 1 (*c*)) which models a terminal respiratory unit, $F(\mu)$ and $G(\mu)$ are those given above with $U = 0$.

4. Effect of interalveolar partitions

Since diffusion dominates convection in the alveoli a detailed study of the gas flow there is unnecessary. A convenient simplification in modelling the respiratory unit is therefore to ignore the interalveolar partitions within the unit. However, some idea of the behaviour of the flow in the individual alveoli may be obtained.

Takematsu (1965) considered Stokes flow in a two-dimensional rectangular cavity of finite depth associated with an imposed velocity along the mouth of the cavity and found that eddies were set up. For a shallow cavity (approximately

square in cross-section) only a single eddy was found but in a deeper cavity more (smaller) eddies were found near the bottom. Takematsu (1966) later reaffirmed this in a study of slow viscous flow past a cavity of infinite depth. Hence it is reasonable that the alveolar walls should reduce the amount of flow and produce some recirculatory flow in the alveoli.

5. Distances of convection

Since nearly all the air in the lung is in the final alveolated regions we assume

$$V_u = V_L/n, \tag{22}$$

where V_u is the air volume of a respiratory unit, V_L is the air volume of the lung and n is the number of respiratory units in the lung.

For the expanding spherical models

$$V(t) = CU_0(t), \tag{23}$$

where V is the velocity of expansion of the unit, U_0 is the mainstream entrance velocity with respect to the sphere and C is a constant. Let $\mathbf{U}$ be the dimensional fluid velocity and $\mathbf{U}^*$ the dimensionless fluid velocity of the quasi-steady flow at any time. Then $\mathbf{U} \approx U_0(t)\,\mathbf{U}^*$. On $\sigma = 0$, $\mathbf{U}$ is in the x direction. Let $\mathbf{U}$ have magnitude $U(x,t)$ and let $\mathbf{U}^*$ have magnitude $U^*(x^*)$, where $x^* = x/L(t)$ and $L(t)$ is the radius of the spherical model at time t.

Then the position of a fluid particle on $\sigma = 0$ is given by

$$x_p(t) = x_p^*(t)\,L(t),$$

and

$$dx_p/dt = U(x_p,t) = U_0(t)\,U^*(x_p^*),$$

$$dx_p/dt = x_p^*(t)\,dL/dt + L(t)\,dx_p^*/dt.$$

Eliminating dx_p/dt from these two equations and using (23) together with $V(t) = dL/dt$ we obtain

$$\frac{dx_p^*}{dt} = \frac{dL}{dt}\left(\frac{1}{C}\,U^*(x_p^*) - x_p^*\right) \times \frac{1}{L}.$$

So

$$\int_{x_1}^{x_2} \frac{ds}{(1/C)U^*(s) - s} = \ln\left(\frac{L_2}{L_1}\right),$$

where a particle at dimensionless position x_1 on the x axis when the radius of the sphere is L_1 moves to position x_2 when the radius is L_2. Using (22) we obtain

$$\int_{x_1}^{x_2} \frac{ds}{(1/C)\,U^*(s) - s} = \tfrac{1}{3}\ln\left(\frac{V_{L_2}}{V_{L_1}}\right),$$

where V_{L_2} and V_{L_1} are the air volumes of the lung corresponding to radii L_2 and L_1. Thus the distance moved by a fluid particle on the x axis between any two lung volumes may be obtained.

6. Physical relevance of the models

If we assume that all units expand at the same constant rate, then, using average entrance velocities based on Weibel's data, we find that U (as defined for expanding spherical models) decreases from about 0·85 at the 20th generation

to zero at the final generation. Note that if the model is not expanding, U is unity and the flow is symmetric. Figure 3 shows streamlines in an expanding sphere for $U = 0{\cdot}75$. We see that except near the wall of the unit, asymmetry of flow is not great.

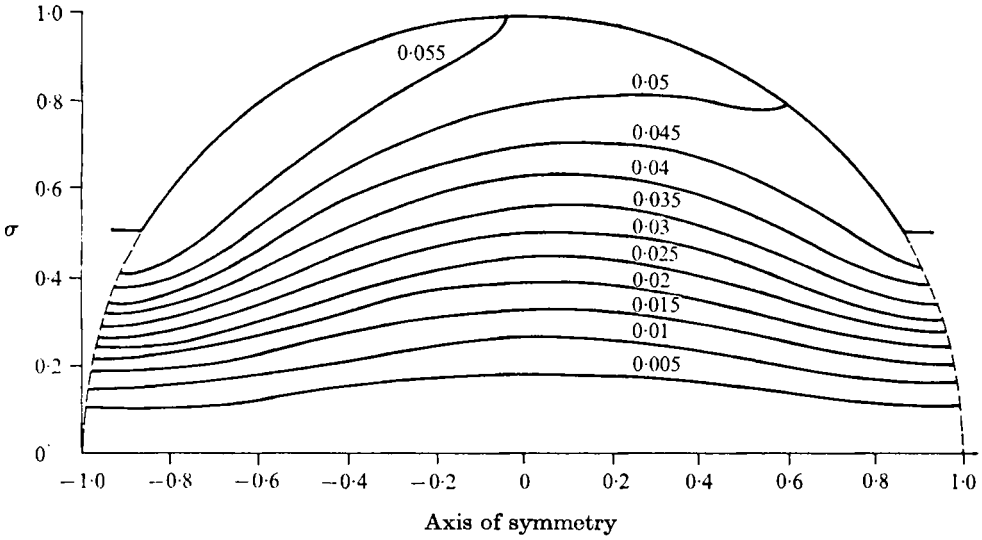

FIGURE 3. Streamlines in spherical model (*a*) (with expanding walls) of a respiratory unit for $b = 0{\cdot}5$ and $U = 0{\cdot}75$.

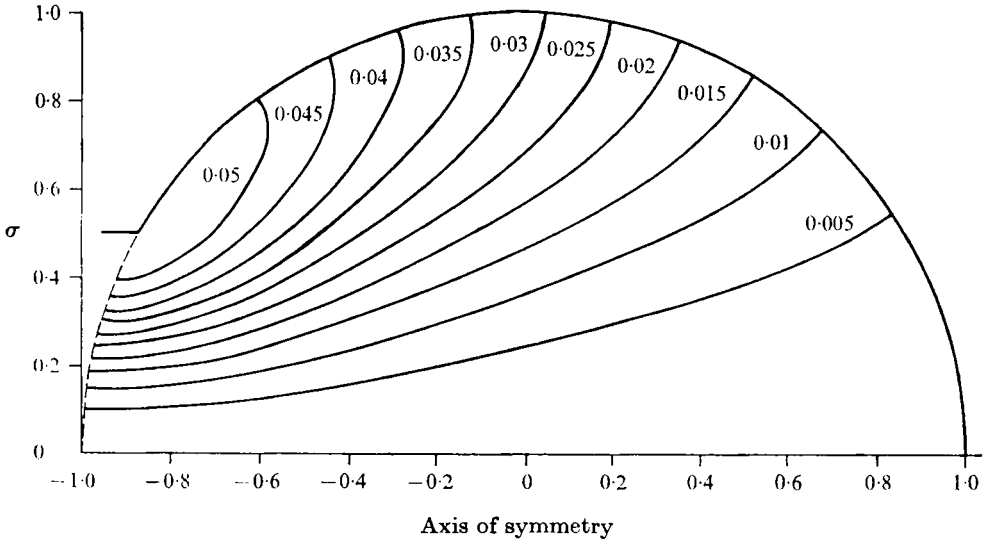

FIGURE 4. Streamlines in spherical model (*e*) (with expanding walls) of a terminal respiratory unit for $b = 0{\cdot}5$.

We have already sacrificed accuracy of description of flow near the wall of a unit by our neglect of interalveolar partitions. It is therefore not unreasonable to base a qualitative discussion of the gross features of the flows on the more convenient

stationary wall models. Of course, in modelling a terminal respiratory unit, mass conservation requires the use of an expanding model.

We have chosen model shapes which in some sense typify a respiratory unit and which are also convenient to study. Although units with fore–aft symmetry are unlikely to occur, asymmetric shapes may be discussed qualitatively in terms of them. Consider a figure of revolution having, say, a spherical shape for $x \leqslant 0$ and the shape of an ellipsoid of revolution for $x \geqslant 0$. We have already shown that

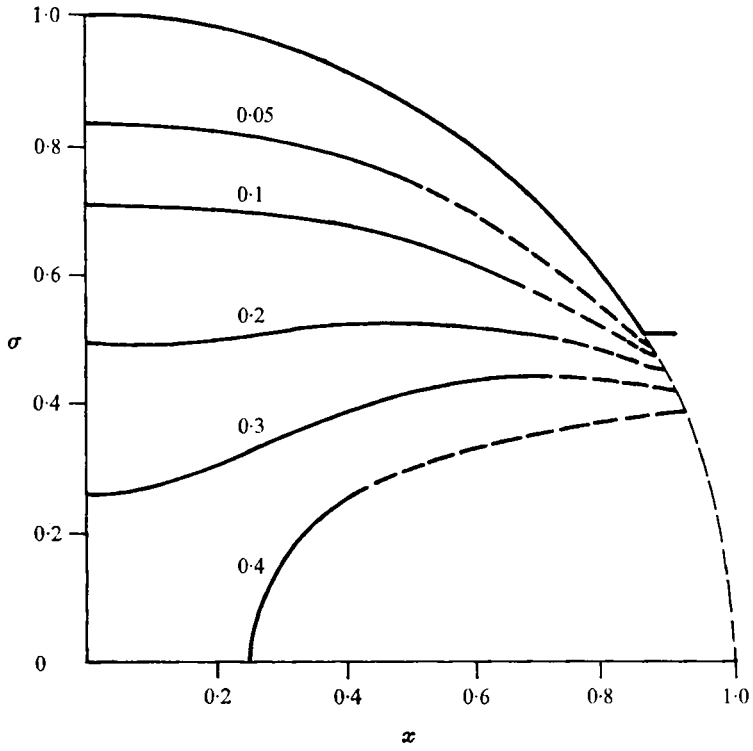

FIGURE 5. Lines of constant velocity in a quadrant of spherical model (*a*) with stationary walls for $b = 0{\cdot}5$. Broken sections of these lines are regions for which velocity data were not obtained.

the flow away from the ends of a figure is not greatly affected by the end conditions and it is known that low Reynolds number flows adjust very easily to variations in shape. We could therefore construct an approximate flow in this asymmetric figure merely by connecting the symmetric flows which exist in the sphere and the ellipsoid of revolution separately.

7. Discussion

For figures 2 (*a*) and (*b*), $b = 0{\cdot}5$ and $0{\cdot}3$ respectively. The length of a unit represented by a sphere is $2(1-b^2)^{\frac{1}{2}}$, so the variation in duct length between figures 2 (*a*) and (*b*) is small (the lengths are 1·7 and 1·9 respectively). Figures 9 (*a*) and (*b*), of course, exhibit no change of duct length, both pairs of flows

indicating that alveoli are better supplied by convection for larger values of b. Larger values of b mean shallower alveoli and hence greater velocities in an alveolus. This is borne out by the velocity profiles in figures 10 (a) and (b). However, the need for maximum respiratory surface area will induce a compromise.

The units in figures 2 (a), 8 and 9 (c) have much greater lengths than those in figures 6 and 9 (a). We see that for the large duct length, transport of air to the

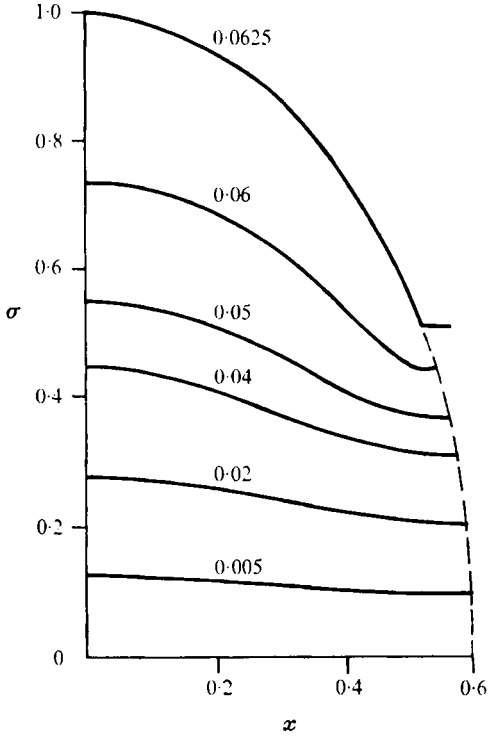

FIGURE 6

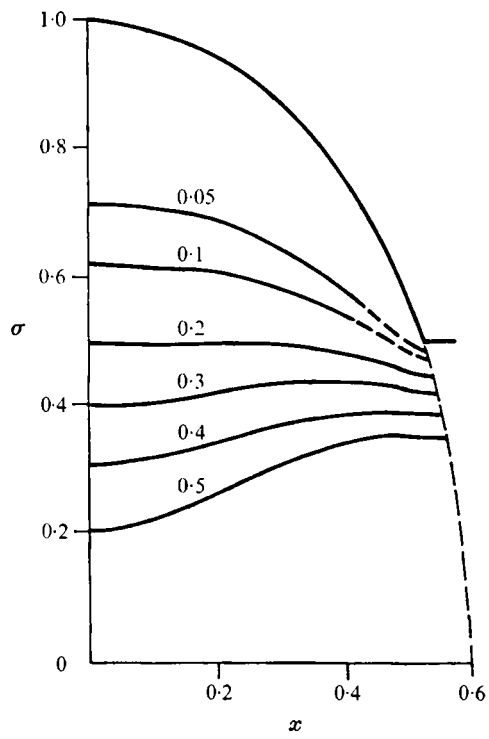

FIGURE 7

FIGURE 6. Streamlines in a quadrant of the oblate ellipsoid of revolution with stationary walls for $b = 0{\cdot}5$ and $c = 0{\cdot}8$.

FIGURE 7. Lines of constant velocity in a quadrant of the oblate ellipsoid of revolution with stationary walls for $b = 0{\cdot}5$ and $c = 0{\cdot}8$. Broken sections of these lines are regions for which velocity data were not obtained.

alveoli by convection is much better; fluid is swept further up towards the alveoli and the velocities there are greater. This second fact is shown clearly by a comparison of the velocity profiles in figures 10 (a) and (c). If we now consider only the circular cylinder model and increase its length even more, there will come a stage where the flow in the central region is Poiseuille and any increase in duct length will merely lengthen the region in which Poiseuille flow dominates. However, the advantages of large duct length shown by our models will be reduced in practice by the increase in the number of alveolar walls which the fluid encounters. These will slow the fluid in the alveoli and reduce the amount of flow through them.

Consider a lung with the small tidal volume of 500 ml where the initial volume V_0 is 2300 ml and the final lung volume V_F is 2800 ml. In such a lung we consider that fluid particle which is on the x axis at the entrance of the model terminal respiratory unit ($x_1 = -(1-b^2)^{\frac{1}{2}}$) when the lung volume is V. If x_2 is the non-

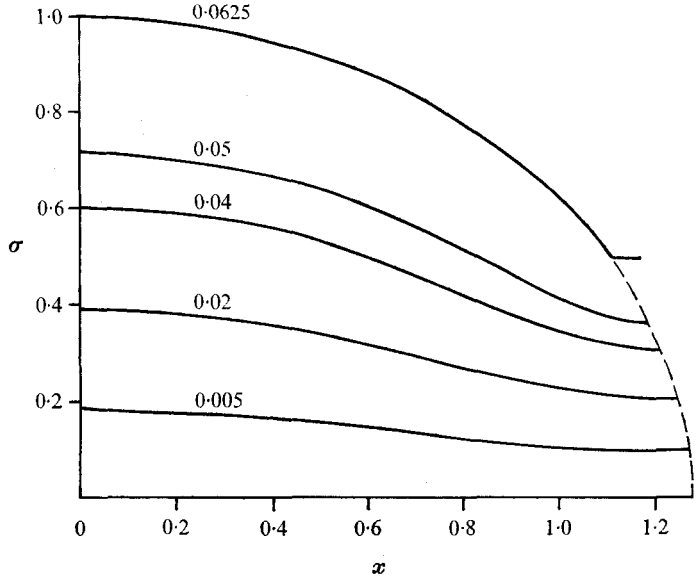

FIGURE 8. Streamlines in a quadrant of the prolate ellipsoid of revolution with stationary walls for $b = 0{\cdot}5$ and $c = 0{\cdot}8$.

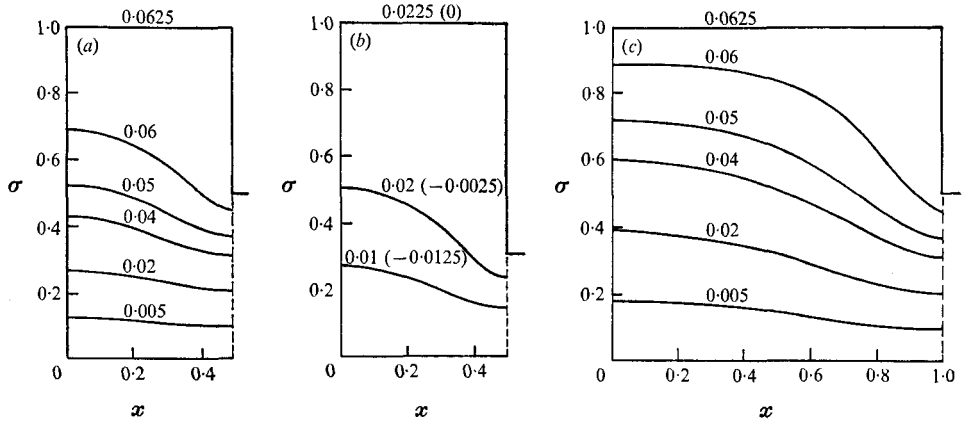

FIGURE 9. Streamlines in a quadrant of the cylindrical model with stationary walls. (*a*) $b = 0{\cdot}5$, $m = 0{\cdot}5$. (*b*) $b = 0{\cdot}3$, $m = 0{\cdot}5$, bracketed numbers are the values of the stream function using the boundary as a reference line, (*c*) $b = 0{\cdot}5$, $m = 1{\cdot}0$.

dimensional position of the particle when lung volume is V_F then $(x_2 - x_1)$ is the dimensionless distance moved by this particle in a sphere of radius unity for an increase $(V_F - V)$ of air volume in the lung. The values of $(x_2 - x_1)$ corresponding to various values of V between V_0 and V_F are given in table 1.

$x_2 - x_1$	V (ml)	$V_F - V$ (ml)
0·83	2300	500
0·73	2400	400
0·62	2500	300
0·49	2600	200
0	2800	0

TABLE 1

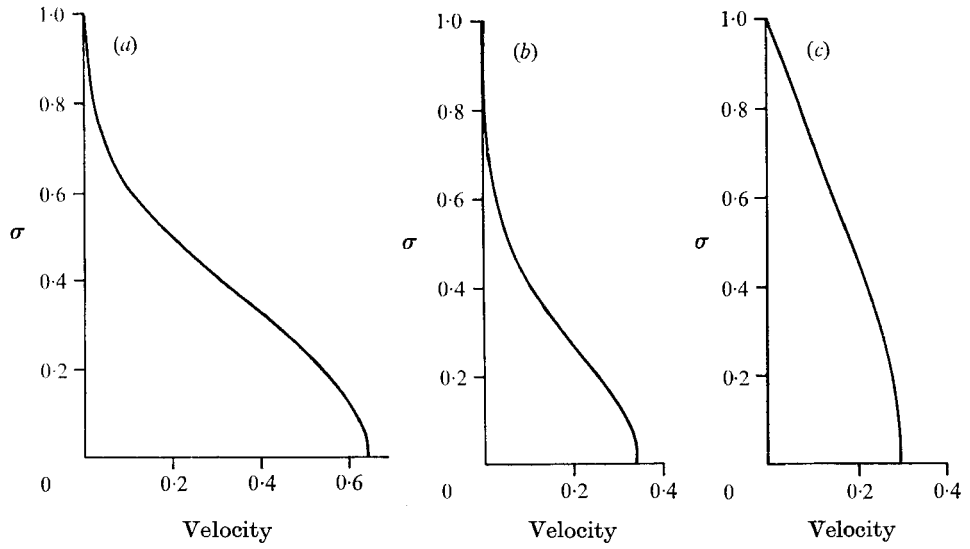

FIGURE 10. Velocity profile at $x = 0$ in the cylindrical model with stationary walls. (*a*) $b = 0{\cdot}5$, $m = 0{\cdot}5$; (*b*) $b = 0{\cdot}3$, $m = 0{\cdot}5$; (*c*) $b = 0{\cdot}5$, $m = 1{\cdot}0$.

Note that the figures are (i) for a small tidal volume and (ii) for a terminal respiratory unit, in which we expect convection to play a lesser role than in units of earlier generation. In spite of (i) and (ii) the figures suggest that convection could be important in the transfer of air through the central core of a unit.

The inspired gas passes through the conducting airways, mixing with dead space gas which has a lower O_2 concentration. So the longitudinal concentration gradient in the final generations may not become large, since a considerable O_2 concentration remains in the alveoli even after expiration. As the incoming breath enters the first-order respiratory units and the O_2 concentration begins to increase, O_2 diffuses more rapidly to the alveolar walls in the immediate vicinity. If subsequent units have to rely predominantly on longitudinal diffusion for their O_2 supply, they may be starved of O_2 in comparison with the first-order units, which have a continual supply by bulk flow. Thus, even though the velocities are small, the concentration of O_2 in the new gas is comparatively high and the net convective transfer generated may be significant when compared with diffusion down the longitudinal concentration gradient. That is, even though the Péclet number is small in the final generations of the lung, it may have less relevance for mass transport in the longitudinal direction than in the radial direction.

Although diffusion is much more important than convection in the radial direction, the flow patterns and velocity profiles in our models suggest that bulk flow could also be of significance in transporting air towards the alveoli, where, of course, diffusion dominates completely.

M. R. Davidson wishes to thank the Australian Commonwealth Government for the financial support of a Commonwealth Postgraduate Award.

REFERENCES

ALTSHULER, B. 1968 Behaviour of airborne particles in the respiratory tract. In *Circulatory and Respiratory Mass Transport, A Ciba Foundation Symposium* (ed. G. E. W. Wolstenholme & J. Knight). London: Churchill.

FITZ-GERALD, J. M. 1969 Ph.D. dissertation, Imperial College, London.

TAKEMATSU, M. 1965 *J. Phys. Soc. Japan*, **20**, 283.

TAKEMATSU, M. 1966 *J. Phys. Soc. Japan*, **21**, 1816.

WEIBEL, E. R. 1963 *Morphometry of the Human Lung*. Springer.

WHITTAKER, E. T. & WATSON, G. W. 1952 *A Course of Modern Analysis*, 4th edn. Cambridge University Press.